SUPPLEMENTARY MATERIAL

Histopathological analyses

The brain of Cases 1 and 3 were removed at autopsy and freshly cut according to an interleaved bi-hemispheric coronal slabbing protocol previously described (Tartaglia *et al.*, 2010). Cerebella were cut into sagittal slabs and brainstems into axial slabs. Following 72-hour formalin fixation, 23 standard regional tissue blocks were obtained from the left cerebral and cerebellar hemispheres and the brainstem. Eight micron-thick formalin-fixed paraffin-embedded sections were obtained from each block and stained with hematoxylin & eosin and with immunohistochemistry for hyperphosphorylated tau, GFAP, amyloid beta, TDP-43, and alpha-synuclein (Tartaglia *et al.*, 2010). NeuN (Synaptic Systems, 1:1000), and non-phosphorylated neurofilaments (SMI32, BioLegend, 1:500). The left cerebral and cerebellar hemispheres and the whole brainstem from case 2 underwent 21-days formalin fixation before block dissection, histological and immunohistochemistry processing as detailed (Tartaglia *et al.*, 2010).

Case 1. The fresh brain weighed 1231 grams. Macroscopically, there was severe atrophy of the STG and moderate cortical thinning of middle frontal gyrus, PCC, and superior frontal sulcus (left greater than right). Moderate hippocampal atrophy was also noted. Microscopically, neuronal loss and gliosis were mostly evident in the entorhinal cortex, STG/MTG, PCC, and AG. Frequent neuritic plaques were found in anterior cingulate cortex, CA1/subiculum, entorhinal cortex, superior/middle temporal gyrus, angular gyrus, and striate cortex. Moderate numbers of neuritic plaques were found in middle insula, claustrum and dentate gyrus. Sparse neuritic plaques were found in putamen and CA3-4. Diffuse plaques were frequent and observed as far caudally as the cerebellar folia (Thal phase 5). There was overall mild cerebral amyloid angiopathy. Severe

neurofibrillary tangle pathology was seen in the ACC, middle frontal gyrus, inferior temporal gyrus, amygdala, CA1/subiculum, entorhinal cortex, precentral gyrus, AG, striate cortex and dorsal raphe (Braak 6). No differences in the severity of neuritic plaque pathology and NFT pathology were seen between cortical areas with or without putative developmental abnormalities. Argyrophilic grain disease limited to the limbic regions was noted. Immunohistochemistry for TDP-43 and alpha-synuclein was negative.

Case 2. The fresh brain weighed 1000 grams. Grossly, there was severe dorsolateral temporal and parietal atrophy, and moderate frontal atrophy. The superior temporal sulcus was grossly widened. The cortical ribbon of the supramarginal and AG were moderately reduced in thickness. Microscopically, the highest extent of neuronal loss and gliosis (severe) was observed in the middle and IFG, and STG/MTG, and to a lesser extent in the PCC and AG. Frequent neuritic plaques were found in anterior cingulate cortex, middle frontal gyrus, inferior temporal gyrus, middle insula, claustrum, putamen, dentate gyrus, CA1/subiculum, entorhinal cortex, superior/middle temporal gyrus, angular gyrus, striate cortex, substantia nigra, tectum, periaqueductal gray, and dorsal raphe. Sparse neuritic plaques were found in CA3-4 and CA2. Diffuse plaques were observed in the cerebellum (Thal phase 5). Mild amyloid angiopathy was observed. Severe NFT pathology was found in the anterior cingulate cortex, middle frontal gyrus, IFG (pars opercularis), inferior temporal gyrus, middle insula, hippocampus, entorhinal cortex, STG/MTG, precentral gyrus, postcentral gyrus, AG, PCC, substantia nigra, tectum and dorsal raphe (Braak 6), and to a lesser extent in other cortical and subcortical regions. The severity of neuritic plaque pathology and NFT pathology was similar between areas with or without cortical dysgenesis. Immunohistochemistry for TDP-43 and alpha-synuclein was negative.

Case 3. The fresh brain weighed 694 grams. There was severe atrophy of the prefrontal, medial temporal, and dorsolateral parietal regions, particularly the left AG. Microscopically, neuronal loss (mild) was mostly severe in the IFG and STG/MTG. Severe gliosis was observed in the IFG, STG/MTG, entorhinal cortex and hippocampus, PCC, AG, amygdala, and locus ceruleus. Immunohistochemistry for beta-amyloid showed frequent neuritic plaques in multiple cortical and subcortical areas and sparse neuritic plaques in the cerebellar folia and brainstem (Thal phase 5), together with abundant diffuse plaques and mild cerebral amyloid angiopathy. Tau immunohistochemistry displayed severe neurofibrillary tangle pathology in the ACC, middle frontal, inferior temporal, precentral, postcentral, AG and striate cortex (Braak 6) as well as in the amygdala, hippocampus, subiculum, and entorhinal cortex, and to a lesser extent in other subcortical regions. Neuritic plaques and NFT burden were similar between areas with or without developmental changes. A large number of Lewy bodies and neurites were observed in the amygdala and to a lesser extent in the hippocampus and substantia nigra. Immunohistochemistry for TDP-43 was negative.

PET imaging

Details about PET data acquisition and tracer synthesis are available in previous publications (Mormino *et al.*, 2008; Villeneuve *et al.*, 2015). Patients underwent ^{11}C-Pittsburg Compound B (PiB)-PET imaging at Lawrence Berkeley National Laboratory (LBNL) on a Siemens ECAT EXACT HR PET scanner (Siemens Medical Systems, Erlangen Germany). A 10 min transmission scan for attenuation correction was obtained before each PET scan. PiB was synthesized at LBNL using a published protocol (Mathis *et al.*, 2003) and ~15 mCi of PiB was injected into an

antecubital vein. Data used in the current analyses was acquired between 50 and 70 min post-injection [i.e. tracer steady state (Ng *et al.*, 2007)] and reconstructed in 5-min frames using an ordered subset expectation maximization algorithm. Images were smoothed with a 4mm Gaussian kernel with scatter correction.

PET frames were realigned, averaged and coregistered onto their corresponding MRI using Statistical Parametric Mapping (SPM) 12. Each patient's MRI was segmented using Freesurfer 5.3 and the resulting cerebellar gray matter region of interest was used to calculate Standardized Uptake Value Ratio (SUVR) images. For each patient, a "PiB index" was derived from the native-space SUVR by averaging the weighted mean value (weighted by size of the ROI) from FreeSurfer-derived regions of interest in frontal, temporal, parietal, and posterior cingulate cortex using the Desikan-Killiany atlas (Desikan *et al.*, 2006). These regions consistently show high PIB retention in studies of AD and aging processing (Villeneuve *et al.*, 2015). PiB-PET SUVR images were visually read as positive or negative for cortical binding (Rabinovici *et al.*, 2011) and SUVR "PiB index" was compared to previously published positivity thresholds based on the same pre-processing (Villeneuve *et al.*, 2015).

For Case 3, major movements were detected during PET acquisition so the SUVR image was calculated based on data acquired between 55 and 60 min post injection.

SUPPLEMENTARY FIGURE 1.

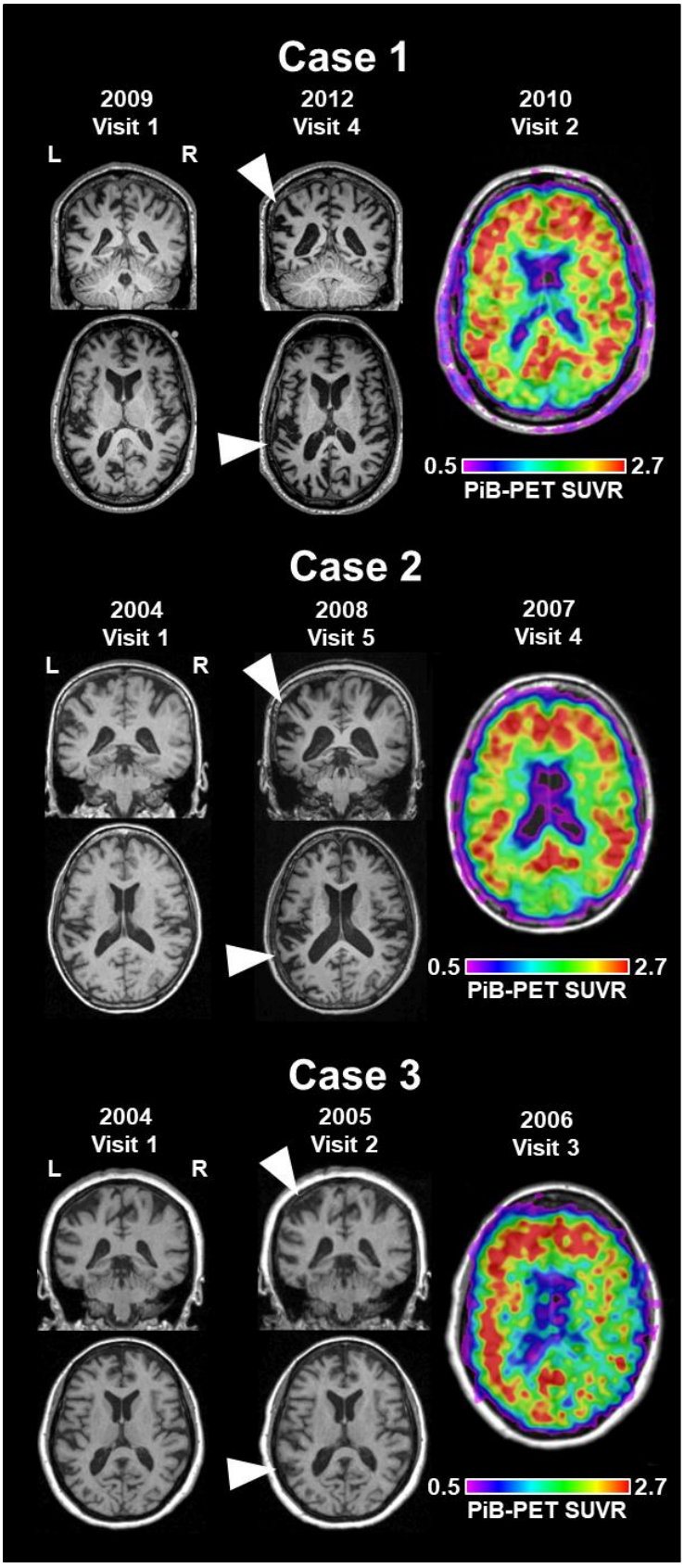

PiB-PET = ^{11}C-Pittsburg Compound B Positron Emission Tomography; SUVR = Standardized Uptake Value Ratio.

Case 1: T1-weighted MRIs annually over a four-year period revealed left greater than right biparietal atrophy with later involvement of frontal and temporal structures including bilateral hippocampi. Amyloid PiB-PET imaging obtained as a part of his second evaluation and showed increased uptake of the PET ligand. SUVR PiB index =2.23.

Case 2: T1-weighted MRIs annually over a five-year period shows relatively isolated left parietal atrophy with notable preservation of frontal and temporal structures including bilateral hippocampi. An amyloid PiB-PET scan obtained during visit 4 was positive for amyloid deposition. SUVR PiB index =2.13.

Case 3: T1-weighted MRIs annually over a two-year period demonstrated progressive deterioration of the left greater than right parietal regions. An amyloid PiB-PET scan obtained during visit 3 was positive for amyloid deposition. SUVR PiB index =2.02.

SUPPLEMENTARY TABLE 1.

	Case 1				Case 2				Case 3		
Age at onset	47				54				40-50		
Age at 1st visit	51				57				53		
Disease duration	11				12				15-25		
Age at death	58				66				65		
Visit #	**1**	**2**	**3**	**4**	**1**	**2**	**3**	**4**	**1**	**2**	**3**
MMSE (30)	26	24	20	4	25	26	23	18	17	12	5
CDR total	0.5	0.5	0.5	1	0.5	1	1	1	0.5	1	1
CDR sum of boxes	2.5	4	4	5	3	4.5	6	7	2.5	4.5	6
Neuropsychological Battery											
CVLT 10min free recall (9)	7	9	5	1	n/a	7	5	6	0	0	n/a
Benson recall (17)	9	9	8	0	15	13	13	10	5	2	0
Digits backwards (9)	3	3	2	2	4	4	2	2	3	2	0
Modified trails (lines/min)	9	9	3	n/a	5	3	3	2	0	0	n/a
Benson copy (17)	16	15	16	1	17	16	17	17	16	4	6
Calculations (5)	4	3	2	1	5	4	4	3	1	0	0
VOSP (10)	10	10	9	n/a	10	9	10	10	6	6	n/a
Language Battery											
Apraxia of speech (7)	0	0	0	0	0	0	0	0	n/a	0	0
Dysarthria (7)	0	0	0	0	0	0	0	0	n/a	0	0
WAB word comprehension (60)	60	60	58	52	60	60	59	57	n/a	52	37
WAB sequential commands (80)	76	72	52	31	68	62	38	45	n/a	37	9
WAB fluency (10)	10	9	6	8	9	9	9	6	n/a	9	6
Semantic fluency (animals in 60 sec)	14	10	4	2	16	18	11	6	8	8	1
Lexical fluency (D words in 60 sec)	10	11	5	2	18	17	10	3	5	4	0
WAB repetition (100)	76	n/a	61	37	80	72	65	54	n/a	75	62
Boston naming (15)	13	12	10	5	14	12	10	4	14	11	12
PPVT-R Total (16)	15	15	14	13	n/a	15	16	14	16	n/a	11
Sentence comprehension (5)	4	1	4	3	n/a	2	3	3	n/a	0	1
Verbal agility (6)	5	3	0	0	n/a	4	2	2	n/a	4	2
Repetition (5)	2	2	1	0	n/a	2	1	1	2	2	1

CDR = Clinical Dementia Rating scale; CVLT = California Verbal Learning Test; MMSE = Mini-Mental State Examination; PPVT-R = Peabody Picture Vocabulary Test Revised; VOSP = Visual Object and Space Perception; WAB = Western Aphasia Battery.

SUPPLEMENTARY TABLE 2.

	Neurodevelopmental Pathological Changes											
	Case 1				Case 2				Case 3			
Language Network	**CDL**	**AN**	**Het. I**	**IntW**	**CDL**	**AN**	**Het. I**	**IntW**	**CDL**	**AN**	**Het. I**	**IntW**
IFG	+	-	+	-	++	+	+	-	+++	+++	+	+
STG/MTG	++	+	-	+	++	+	+	-	++	++	++	+
AG	++	++	+	+	++	-	-	-	+	++	+	-
Control Regions												
ACC	-	-	-	-	-	-	-	-	++	+	-	-
Insula	-	-	+	-	-	-	-	+	+	+	+	-
PCC	+	-	-	-	+	-	+	-	+	+	++	-
	Alzheimer's Disease Pathological Changes											
Language Network	**NL***	**Gliosis**	**NFT**	**NP**	**NL***	**Gliosis**	**NFT**	**NP**	**NL***	**Gliosis**	**NFT**	**NP**
IFG	-	++	+++	+++	+	+++	+++	+++	+	+++	+++	+++
STG/MTG	-	+++	+++	+++	+	+++	+++	+++	+	+++	+++	+++
AG	-	+++	+++	+++	-	+++	+++	+++	-	+++	+++	+++
Control Regions												
ACC	-	+	+++	+++	-	+	+++	+++	-	++	+++	+++
Insula	-	++	+++	++	-	+	+++	+++	-	+	+++	+++
PCC	-	+++	+++	+++	-	+++	+++	+++	-	+++	+++	+++

NL: neuronal loss, NFT: neurofibrillary tangles, NP: neuritic plaques, CDL: cortical dyslamination, AN: atypical neurons, Het. I: heterotopic neurons in cortical layer I, IntW: tau-immunoreactive interstitial white matter neurons.

- = none, + = sparse, ++ = moderate, +++ = severe.

*Neuronal loss is characterized in a semi-quantitative manner and is only positive if greater than 50% of neurons in a high-power field are lost.

REFERENCES

Desikan RS, Ségonne F, Fischl B, Quinn BT, Dickerson BC, Blacker D, et al. An automated labeling system for subdividing the human cerebral cortex on MRI scans into gyral based regions of interest. Neuroimage 2006; 31: 968-80.

Mathis CA, Wang Y, Holt DP, Huang G, Debnath ML, Klunk WE. Synthesis and evaluation of 11C-labeled 6-substituted 2-arylbenzothiazoles as amyloid imaging agents. J Med Chem 2003; 46: 2740-54.

Mormino E, Kluth J, Madison C, Rabinovici G, Baker S, Miller B, et al. Episodic memory loss is related to hippocampal-mediated β-amyloid deposition in elderly subjects. Brain 2008; 132: 1310-23.

Ng S, Villemagne VL, Berlangieri S, Lee ST, Cherk M, Gong SJ, et al. Visual assessment versus quantitative assessment of 11C-PIB PET and 18F-FDG PET for detection of Alzheimer's disease. J Nucl Med 2007; 48: 547-52.

Rabinovici GD, Rosen HJ, Alkalay A, Kornak J, Furst AJ, Agarwal N, et al. Amyloid vs FDG-PET in the differential diagnosis of AD and FTLD. Neurology 2011; 77: 2034-42.

Tartaglia MC, Sidhu M, Laluz V, Racine C, Rabinovici GD, Creighton K, et al. Sporadic corticobasal syndrome due to FTLD-TDP. Acta Neuropathol 2010; 119: 365-74.

Villeneuve S, Rabinovici GD, Cohn-Sheehy BI, Madison C, Ayakta N, Ghosh PM, et al. Existing Pittsburgh Compound-B positron emission tomography thresholds are too high: statistical and pathological evaluation. Brain 2015; 138: 2020-33.